Analysis of the aftertreatment performance in HD-SI engine fueled with LPG

Vicente Bermúdez[1]*, Santiago Ruiz[1], Brayan Conde[1] and Lian Soto[2]

[1]Universitat Politècnica de València, CMT-Motores Térmicos, Camino de Vera s/n, 46022 Valencia, Spain

[2] Bertrandt AG, Pol. Industrial Rosanes. Carrer França,15-25, Barcelona, Spain

*Corresponding author. Tel.: +34 96387-9652; E-mail: bermudez@mot.upv.es

Abstract

This research/article aimed to analyze the influence of an after-treatment system (ATS) on emissions of a heavy-duty spark-ignition (HD-SI) engine fueled with liquified petroleum gas (LPG), in the context of current Euro VI emissions requirements. The ATS is composed by a three-way catalyst (TWC) in series with a diesel particle filter (DPF). Emissions testing were carried out on an engine test bench according to homologation procedures, performing both world harmonized stationary cycle (WHSC) and world harmonized transient cycle (WHTC), to study the effects of the engine operating parameters on pollutant emissions behavior and ATS performance during steady and dynamic states, respectively. Instruments used were a gas analyzer Horiba MEXA ONE to measure gaseous emissions, HORIBA OBS ONE PN to measure particle matter (PM) concentration, and spectrometer TSI EEPS 3090 to measure PM concentration and particle size distribution (PSD). The results showed some important aspects such as the effects of engine speed and load on pollutant emissions formation and ATS performance, the influence of the three-way catalyst (TWC) on particulate matter (PM) reduction due to the relationship between volatile unburned hydrocarbons (UHC) and the emergence of nucleation-mode particles, stressing that ATS implementation is mandatory to meet the current emissions requirements.

Keywords: After-treatment system, DPF, HD-SI, gas engine, LPG, pollutant emission, PM, PSD, TWC.

1. Introduction

The pollutant emission standards in internal combustion engines (ICEs) are increasingly stringent, due to the interest of governments to create social awareness about the effects of these emissions on health and environment.[1] In this sense, the automotive sector has focused on the development of different methodologies and technologies to meet the demanding limits established by the current Euro VI standards.[2] Euro VI regulates the emissions of the following pollutant compounds: unburned hydrocarbons (UHC), carbon monoxide (CO), nitrogen oxides (NOx), and particulate matter (PM).

In general, methodologies for reductions of pollutants can be classified into two groups. The first group pertains to active solutions that affect engine design and its components, such as the optimization of injection systems[3], improvements in the air management process[4], new concepts of low-temperature combustion (LTC)[5], and the use of alternative fuels[6]. The second group involves passive solutions to reduce pollutant compounds across the exhaust line with the use ATS[7]. For example, the three-way catalyst (TWC) allows oxidate and reduce gaseous pollutant compounds[8], while the particle filter reduces the PM emission[9].

The fuel type has a direct influence on the pollutant compounds emergence. In this sense, ICE fuels must be in liquid or gaseous, not solid phases because of combustion engines' high engine operating speeds.[10] The main advantage of liquid fuels is their high energy densities[11,12]. Liquid fuels do, however, depend upon ICE-external systems to inject fuel at high pressures into engines' combustion chambers in the form of fuel/oxidant aerosols.[13] Gas-phase fuels, in contrast, mix with oxidants much more readily than do liquid fuels. This allows combustion to occur at comparatively lower temperatures, and, consequently, with less pollutant emissions[14].

Many researchers[14–17], discuss the various advantages of engines that use gas-phase fuels over the more ubiquitous gasoline or diesel engines. One such benefit is that gas-powered engines' thermal efficiency is greater than that of gasoline or diesel engines.[18] Furthermore, due to its lower pollutant emission, gas-powered engines meeting current and even future regulations with less complex ATS[19]. However, as mentioned earlier, despite gas engine advantages respect to engines powered by gasoline or diesel, these engines depend on ATS implementation too, in order to meet with the current regulation standards[9].

The engine ATS generally consists of two devices the catalyst, and the particle filter. TWC is the best alternative to oxidize and reduce gaseous compounds in spark-ignition (SI) engines. due to its higher effectiveness in a stoichiometric equivalence ratio range[20]. While DPF function is to decrease PM emissions to the environment. It is worth mentioning that, although PM emission is a problem present in both engine types, these emissions were first regulated in the compression ignition (CI) engines. Hence, the studies related to particle filters have been focused first on DPF development[21] and after in gasoline particle filter (GPF)[22]. Accordingly, results obtained from those researches are being used for ATS evolution in alternative fueled engines[23].

In addition to the investigations mentioned above, numerous studies have shown the relationship between ICE emissions with health problems[24,25] and environmental deterioration[26]. For example, CO can cause death in high concentration because this compound mix with the blood faster than oxygen, UHC are usually composed by polycyclic aromatics (PAH) guilty of carcinogenic problems; the NOx are responsible for acid rain, photochemical smog, and ozone reduction. Also, PM emitted by the ICEs are composed of particles with different characteristics and properties according to their size, chemical composition, solubility, and origin[4,27]. Consequently, they are the focus of different scientific research that involve particles of diameter less than 1 μm.[28] Since such particles can persist for up to one week in the atmosphere, they can penetrate the human lungs and lodge in the alveoli, which can cause various forms of lung or cardiac cancers [29].

As matter of fact, PM emissions are composed of an insoluble organic fraction (IOF) and a soluble organic fraction (SOF), in the case of the IOF, its main compounds are dry soot and sulfates, while the SOF, is mainly composed of acetylenes and polycyclic aromatics (PAH)[30] that come from the fuel and the lubricant[31] One of the methodologies used to study the behavior of PM emission is the particle size distribution (PSD) which generally shows a bimodal structure[32]. The nucleation-mode in PSD brings together those particles with sizes between 5 to 30 nm, composed of condensed volatile or semi-volatile material, which through the nucleation forms new particles of greater mass with some solid parts of metal and carbon. Similarly, accumulation-mode brings together particles with sizes between 30 nm to 1μm made up for agglomerate of soot particles, whose surface contains volatile material absorbed during its formation.[33]

According to the previous considerations, the main objective of this paper was to analyze experimentally the effects of TWC and DPF on pollutants emitted by an LPG-fueled engine. For this purpose, the homologation cycles, WHSC and WHTC, were used for the engine tests. First, WHSC was employed to study pollutant emissions, PSD, and the ATS efficiency on eight steady-state modes. Furthermore, the operating modes were separated into two groups under their load percent, those modes with a load lower than 50% were grouped in the first group, while modes with a load higher or equal to 50% were grouped in the second one, in order to facilitate the analysis of the results. Latterly, WHTC was used to study the effects of engine transient-states on pollutant emissions emergence as well as the influence of TWC and DPF on pollutant reduction. All results made evident the need for ATS implementation at the time of homologating the engine under the current Euro VI. The instruments HORIBA MEXA-ONE, HORIBA OBS-ONE PN, and TSI-EEPS 3090 were used for pollutant measurement of gaseous compounds, PM concentration, and PSD during tests described above.

2. Material and methods

The main characteristics of the engine and the most relevant properties of the LPG fuel are discussed in this section along with a description of the different devices used for pollutant emission measurement and test methods.

2.1. Engine and Fuel Properties

The engine used in this study was an 8-cylinder, heavy-duty (HD) spark-ignition (SI) with 7.2 l displacement including ATS composed by TWC system and DPF downstream, which complies with Euro VI standards. This engine is mounted in a typical passenger bus, and detailed specifications of the engine are given in Table 1.

Table 1. LPG engine main characteristics

Characteristic	Value
Style	4 stroke, HD-SI Engine
Emission standard	EURO VI
Maximum power	221 kW@2250 rpm
Maximum brake torque	1070Nm@1890 rpm
Maximum injection pressure	12 bar
Injector type	Peak and Hold
Number of valves per cylinder	2
Total displaced volume	7200 cm^3
Number of cylinders	8
Compression ratio	11.2:1

Commercial LPG fuel was employed during the experiments presented in this study. The main fuel physicochemical properties are provided in Table 2.

Table 2. Physical and chemical properties of LPG fuel**.**

Properties	Value
% C_3H_8	92.81
% C_4H_{10}	4.35
Density [kg/m^3] (T=15°C)	560
Viscosity [cSt] (T=40°C)	57.3
RON [-]	105
(A/F) ratio	15.5
Vaporization temperature [°C]	-42
Lower heating value [MJ/kg]	46.1

2.2. Experimental setup

The engine was connected to a Horiba HT460 asynchronous dynamometer, which allowed instant torque and speed control. Furthermore, all instrumentation used for the measure of air mass flow, fuel mass flow, torque, and speed are summarized in Table 3.

Table 3. Characteristics of engine instrumentation**.**

Magnitude	Sensor/ Instrument	Range	Error
Mean pressure	Piezoelectric Pressure sensor	0-70 bar	± 1%
Air mass flow	AVL Flowsonix Air	0-±2400 (kg/h)	± 1%
Fuel mass flow	Emerson Coriolis micro motion	0-2180 (kg/h)	± 0.35%
Temperature	Thermocouple Type K	-200-1, 200 (°C)	±2.5°C
Torque	Torquimeter HBM T40	0-2000 (Nm)	±0.05%

Figure 1 shows the analyzers used in this study to measure the pollutant emissions in the following three positions across the after-treatment system: 1) output of the engine without ATS, 2) after TWC, and 3) after DPF. In this sense, the devices Horiba MEXA-ONE for the gaseous compounds, Horiba OBS-ONE PM for PM concentration with diameters between 23 nm and 1 μm, and the EEPS-TSI 3090 for PM concentration and PSD with diameters between 5.6 nm and 560 nm were employed to evaluate emissions on each ATS position.

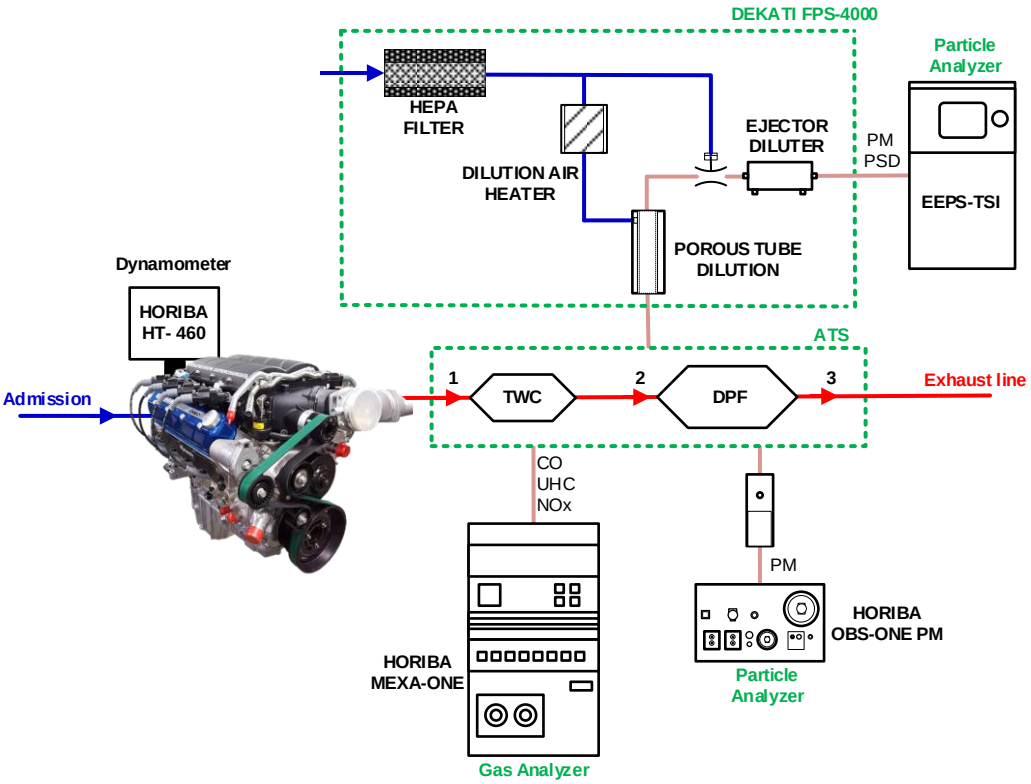

Fig. 1. Experimental setup for the evaluation of pollutant emissions.

In addition, in order to measure PM concentration and PSD, two different dilution systems were employed. The first one was the Horiba OBS-ONE PM integrated system, and it had a double dilution system with a total dilution grade of one hundred, while the EEPS-TSI 3090 was connected to the Dekati FPS 4000 in order to allow sample flowed across the isothermal primary diluter (A to B way in Fig. 2), which was a porous tube (PTD), and a subsequent ejector diluter (ED) acts as the secondary diluter (B to C way in Fig. 2) before entering the EEPS-TSI 3090.

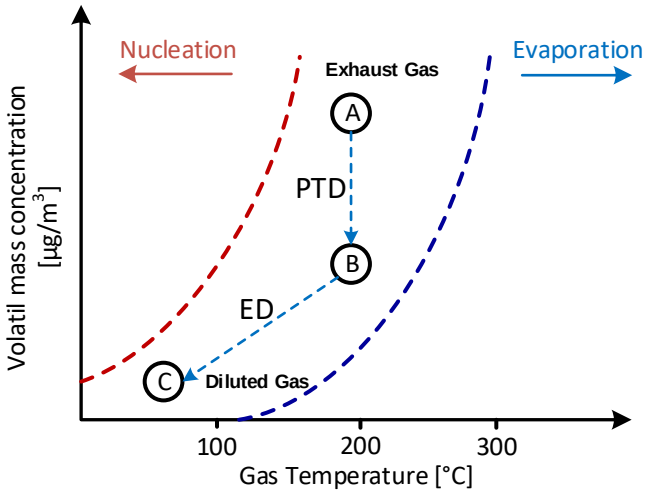

Fig. 2. Particle evolution at dilution system. Theoretical phase-diagram used in the methodology for measuring particle size distribution[34].

In order to give a detailed characterization of the instruments used, Table 4 shows the range and the measurement sensitivity of each pollutant measured.

Table 4. Characteristics of pollutant equipment

Pollutant emission	Instrument	Range	Sensitivity
CO_2	Horiba MEXA-ONE - NDIR	0-0.5 to 0-20 (vol%)	± 1% (full scale)
CO_L	Horiba MEXA-ONE - NDIR	0-50 to 0-5000 (ppm)	± 1% (full scale)
CO_H	Horiba MEXA-ONE - NDIR	0-0.5 to 0-12 (vol%)	± 1% (full scale)
NOx	Horiba MEXA-ONE - CLD	0-10 to 0-10000 (ppm)	± 1% (full scale)
UHC	Horiba MEXA-ONE - HFID	0-50 to 0-60000 (ppmC)	± 1% (full scale)
PM (23nm-1μm)	HORIBA OBS-ONE PM	$5{\cdot}10^7$ (#/cm^3)	± 1% (full scale)
PM (5.6nm-560nm)	TSI-EEPS	5.6 nm: 10^8 (#/cm^3) 560 nm: 10^6 (#/cm^3)	± 5% (actual value)

2.3. Calculation methods

The method adopted for the calculation of after-treatment systems efficiency (ATS_{eff}) was based on Equation (1). In this equation, S_{e-down} and S_{e-up} are the measurement values of the pollutants downstream and upstream the after-treatment system setup.

$$ATS_{eff} = 100 - \frac{S_{e-down}}{S_{e-up}} \cdot 100 \quad (1)$$

However, the results present in this study were focused on creating two groups with particle dimeter size lower and upper to 23 nm, similar to the investigation by *Napolitano et al*[9]. All foregoing motivated by current regulations and projecting the study to future restrictions. *Seinfeld et al*[35] established that PSD is the all groups sum and his calculation is shown in the Equation (2) assuming the log-normal size distribution function.

$$\frac{dN_i}{d\log dp_i} = \frac{1-x}{\sqrt{2\pi}\log\ \sigma_{g1}} \cdot e^{-\frac{log^2\left(\frac{dp_1}{dp_{g1}}\right)}{2\,log^2\sigma_{g1}}} + \frac{1-x}{\sqrt{2\pi}\log\sigma_{g2}} \cdot e^{-\frac{log^2\left(\frac{dp_2}{dp_{g2}}\right)}{2\,log^2\sigma_{g2}}} \quad (2)$$

In Equation (2) *x* is the ratio of the total concentrations number of two distributions, d_{p1}, d_{p2}, d_{pg1}, d_{pg2}, σ_1 and σ_2 are the geometric mean diameters, median diameters, and geometric standard deviations of each peak, and N_i is the particle concentration of particle size d_{pi}. The fit was achieved by minimizing the mean square error function by means of the Nelder–Mead simplex method.

$$N_{mode} = \sum_{dp(low)}^{dp(up)} dN_i \quad (3)$$

Furthermore, to calculate the different particle-mode concentrations (N_{mode}), Equation (3) was used. In this equation, $dp_{(up)}$ and $dp_{(down)}$ are the particle size limits defining the range of the diameters for each mode. The following decomposition was considered:

- First mode (N_1.): particle sizes from $dp_{(down)}$ = 5.6 nm to $dp_{(up)}$ = 23 nm.
- Second mode (N_2.): particle sizes from $dp_{(down)}$ =23 nm to $dp_{(up)}$ = 560 nm.
- Finally, the Total mode (N_{Tot}.) particle concentration was considered from $dp_{(down)}$ = 5.6 nm to $dp_{(up)}$ =560 nm.

2.4. Test schedule

Eight different operation modes were chosen among operation modes from the WHSC displayed in Table 5, in order to get representative results of ATS performance in a wide range of engine speed and load, discarding the modes one and thirteen due to their poor relevant with zero percent of the load. As well as the full load modes (two, five, and ten) because of their lower time length respect to the required time required by the PSD measurement instrument.

Table 5. WHSC test modes

Mode	Speed [%]	Load [%]	Mode length [s]
1	0	0	210
2	55	100	50
3	55	25	250
4	55	70	75
5	35	100	50
6	25	25	200
7	45	70	75
8	45	25	150
9	55	50	125
10	75	100	50
11	35	50	200
12	35	25	250
13	0	0	210

According to previous considerations, the behavior of the next engine parameters: speed, torque, power (Pe), and BSFC are illustrated in Figure 3, along with the position of each operation mode from the WHSC selected for testing.

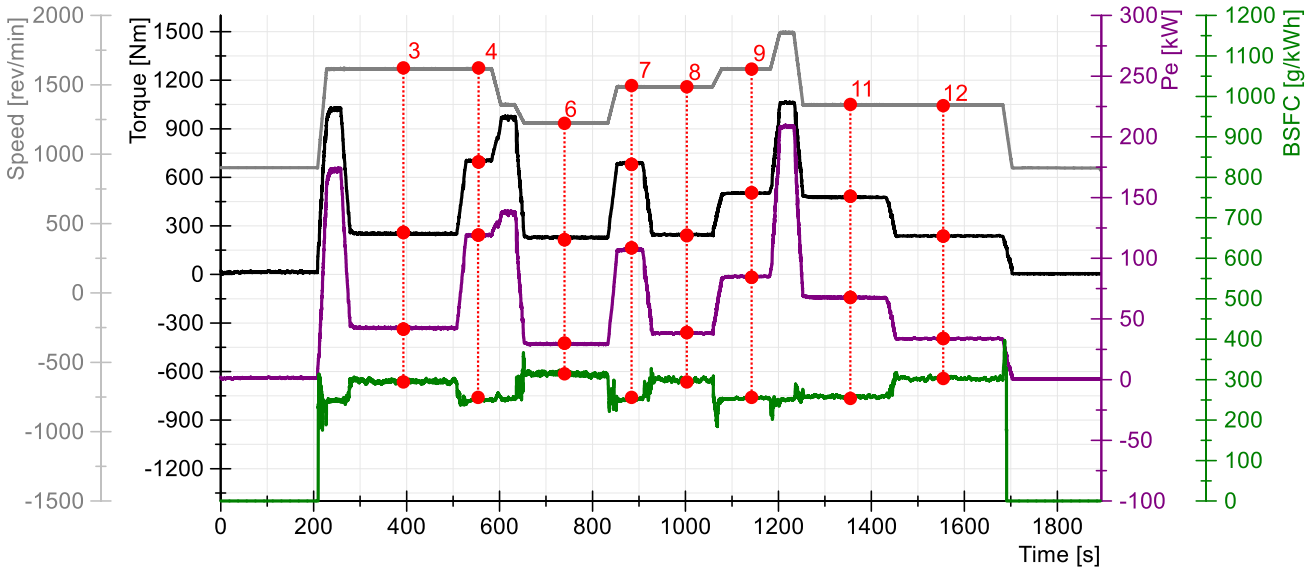

Fig. 3. Main test parameters from WHSC and state points selected.

Finally, similar to the methodology used for the engine steady-states study described previously. The WHTC, whose speed and torque are shown in Figure 4, it was employed for the evaluation of ATS performance under engine transient states.

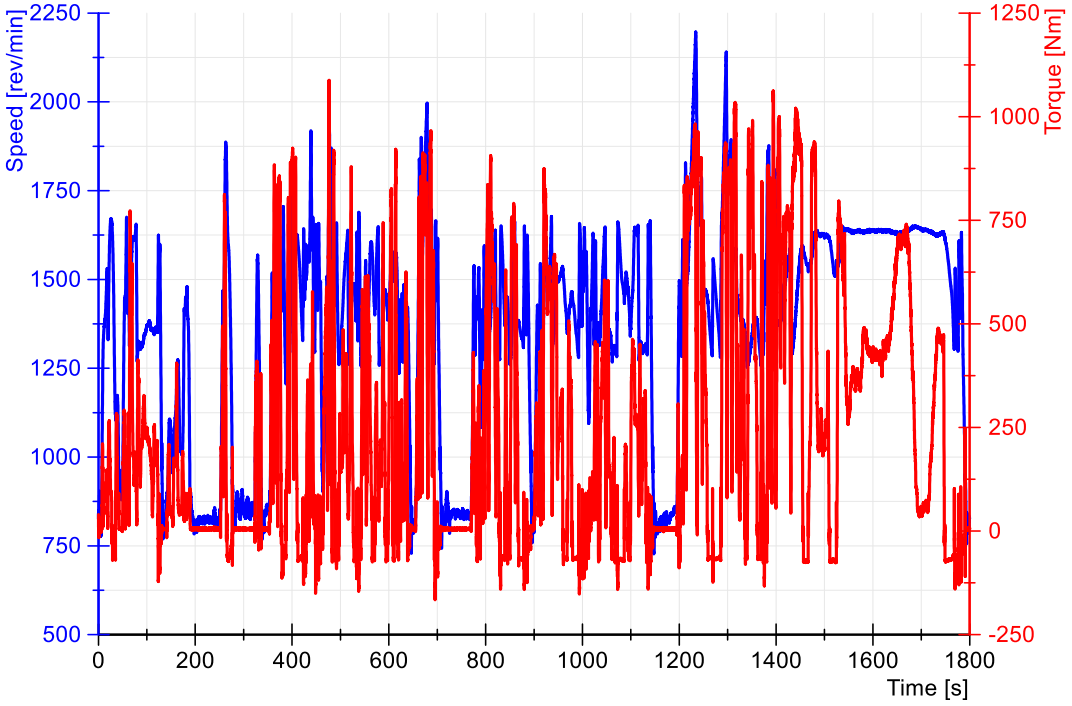

Fig. 4. Engine speed and torque across the WHTC

2.4.1. Methodology test

For testing ATS performance and pollutant emissions behavior in the three locations, shown in Figure 1. The measurement instruments were placed first on the engine output while performing the cycles WHSC and WHTC, in accordance with the sequency set out in Figure 5, and subsequently, the location of all measurement instruments was changed, with aim of analyzing the other two positions (after TWC and after DPF), according to directions as below:

- The engine was run at reference steady-state operating point with 50% of speed and load. The time until performing the tests was determined by the variation at TWC outlet temperature. In this sense, when this temperature was stable, both cycles, first the WHSC and later the WHTC, were carried out.
- When both cycles had been assessed, the engine was taken to reference steady-state point again, and the second reference was measured.
- The test of second and third positions across the exhaust line were performed in the same way that the first one.

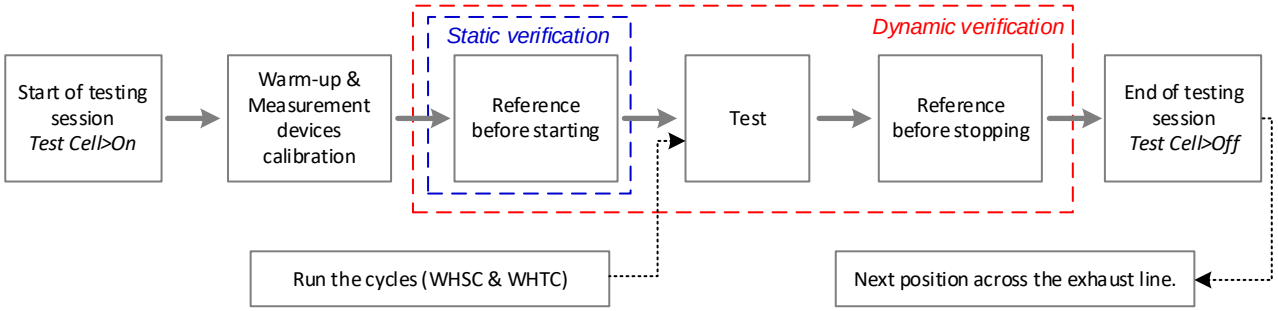

Fig. 5. Methodology employed for testing of ATS performance in the engine steady and transient states.

3. Results and discussion

This section includes various test results. They pertain to gaseous emissions, aftertreatment efficiencies, and analyses of particulates in steady and transient engine states.

3.1. Results for engine parameters

As noted above, in order to study the pollutant emission behavior and ATS performance during engines' steady states, eight modes from the WHSC cycle were selected. They, in turn, are divided into two groups. The first group is comprised of modes whose load percentage is less than 50%, while the second group subsumes those modes whose load is greater than or equal to 50%. Figure 6 shows the equivalency ratio and exhaust gas temperatures for each of the two modes to allow an analysis of how engine parameters affect ATS efficiency.

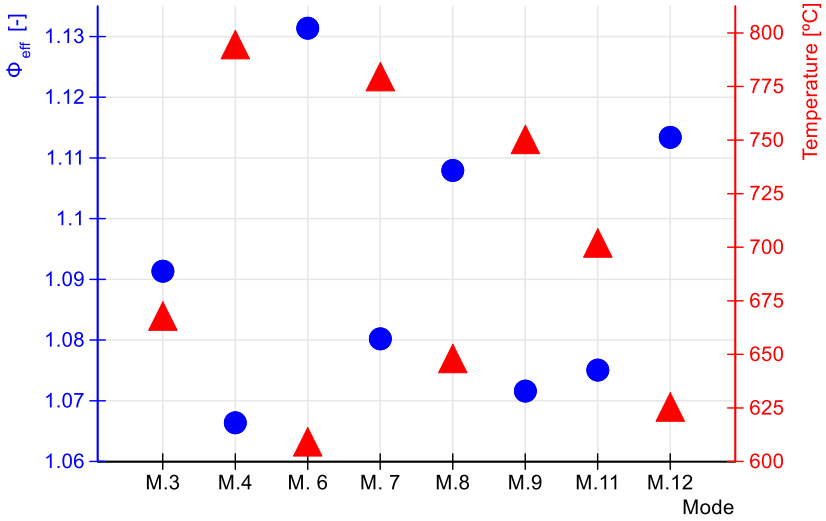

Fig. 6. Engine equivalency ratios and temperatures of exhaust gases on engines' steady-state conditions

As per Table 5, the first group consists of modes three, six, eight, and twelve, while modes four, seven, nine, and eleven belong to the second group. Figure 6 shows that modes with higher equivalence ratios have relatively lower exhaust gas temperatures. The information in Figures 5 and 6 permits evaluating the following four statements:

- Efficiencies of ATS devices depend upon both equivalency ratios and exhaust gas temperatures[36,37], exhaust gas temperatures, in turn, depend upon engine loads[38,39].
- Equivalency ratios influence the formations of some gaseous compounds, such as CO and UHC, whose formative processes are favored in rich mixtures (high equivalency ratios), and lean mixtures (low equivalency ratios), respectively[40,41].
- NOx can be formed only at high temperatures, unlike the other two gaseous pollutants, which are more dependent upon the equivalency ratio [40,42].
- The PM formation depends upon the same measure of low equivalency ratio and high temperature during the combustion process [40,43].

The next sections are predicated upon the information above. They present the results of pollutant emissions and ATS efficiency during steady engine states.

3.2 Results for steady-state engine conditions

Steady-state results are divided into two parts. Section 3.2.1 is an analysis of gaseous emissions and efficiencies of the ATS devices efficiencies, while Section 3.2.2's results concerning ATS devices focus only upon PM emissions.

3.2.1. Results for gaseous compound emissions

The graphs and charts presented in Figure 7 show the pollutant gases behavior on the three points across the exhaust line as well as the efficiency of ATS devices for each operating mode selected from WHSC.

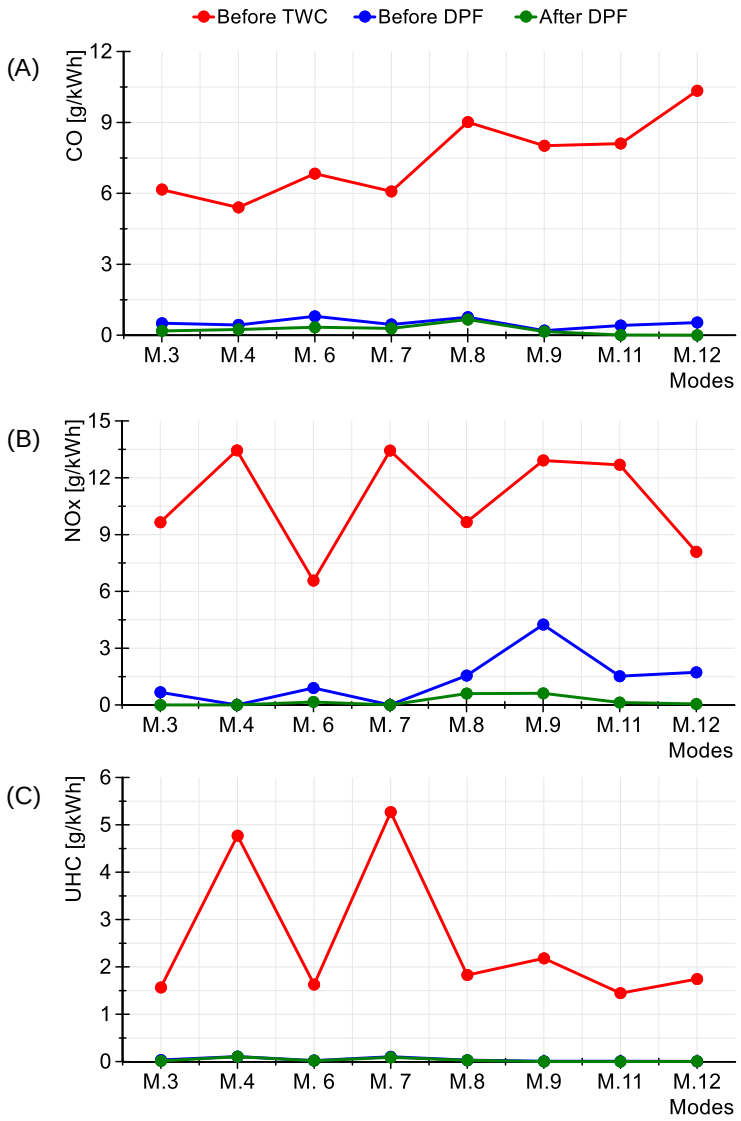

	Eff_TWC [%]	Eff_DPF [%]	Eff_ATS [%]
Mode 3	91.75	64.02	97.03
Mode 4	91.97	44.04	95.51
Mode 6	88.29	57.95	95.08
Mode 7	92.54	36.30	95.24
Mode 8	91.55	13.02	92.65
Mode 9	97.53	23.04	98.10
Mode 11	94.91	98.13	99.91
Mode 12	94.81	99.97	100.00

	Eff_TWC [%]	Eff_DPF [%]	Eff_ATS [%]
Mode 3	93.03	99.78	99.98
Mode 4	99.99	14.32	99.99
Mode 6	86.31	82.14	97.56
Mode 7	99.99	16.14	99.99
Mode 8	83.94	61.08	93.75
Mode 9	67.13	85.44	95.21
Mode 11	88.00	91.35	98.96
Mode 12	78.68	96.89	99.34

	Eff_TWC [%]	Eff_DPF [%]	Eff_ATS [%]
Mode 3	97.77	60.17	99.11
Mode 4	97.77	1.91	97.81
Mode 6	98.59	17.01	98.83
Mode 7	98.03	14.11	98.31
Mode 8	98.46	12.46	98.46
Mode 9	99.69	72.37	99.91
Mode 11	99.44	98.36	99.44
Mode 12	99.61	14.91	99.67

Fig. 7. Gaseous emissions of the steady-state modes selected from the WHSC.

Figure 7A shows the behavior of CO emissions in each selected operating mode. It demonstrates, for example, that CO emissions increase with engine loads' decreases, and that the temperature influence TWC efficiency where the operation modes with a lower temperature (M3, M6, M8, and M12) show a lower efficiency of the TWC also, while modes with higher temperature and percent of load medium or high (M4, M7, M9, and M11) showed generally a better efficiency of the ATS on CO emissions.

Figure 7B shows that the behavior of NOx emissions and the efficiency of ATS devices highlighting findings such as NOx emission was generally greater than the other gaseous compounds in all operating modes. Furthermore, modes with medium or high loads show higher temperatures, so therefore NOx emissions were higher. However, it must be noted that the highest temperatures occur in modes four and seven. Although NOx emissions were relatively elevated in these modes, the TWC efficiency was better.

Finally, Figure 7C shows that UHC emissions were the lowest in all operating modes. As expected, the relatively low equivalency ratios of modes four and seven demonstrate high UHC emissions[44]. Notwithstanding, we must not overlook the efficiency (greater than 97%) of TWC regarding UHC emissions in each mode evaluated, independently of exhaust gas temperature.

3.2.2. Results for particulate matter emissions

In this section, the results obtained from the evaluation of ATS efficiency, using the TSI-EEPS 3090 and after analyzing PM concentration and PSD for each one of the positions across the exhaust line, are presented. The behaviors of all factors studied for each operating mode appear in Figure 8. Operation modes have been divided

into two groups. The first consists of modes with a low load (Figure 8A), while modes with a medium and high load comprise the second group (Figure 8B).

PN_Total [#/cm³]	PN_6-23 [#/cm³]	PN_23-560 [#/cm³]	Eff. Total [%]	Eff. 6-23 [%]	Eff. 23-560 [%]
3.63E+05	1.33E+05	2.30E+05	42.8	15.3	58.8
2.08E+05	1.13E+05	9.48E+04	87.1	88.2	85.8
2.68E+04	1.34E+04	1.35E+04	92.6	90.0	94.1

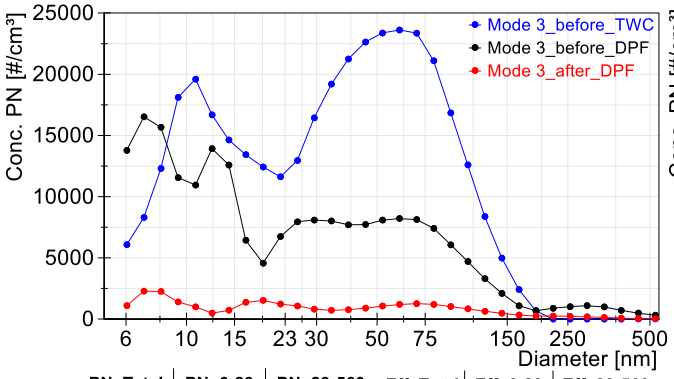

PN_Total [#/cm³]	PN_6-23 [#/cm³]	PN_23-560 [#/cm³]	Eff. Total [%]	Eff. 6-23 [%]	Eff. 23-560 [%]
2.21E+05	1.20E+05	1.01E+05	66.6	69.9	62.6
7.39E+04	3.63E+04	3.76E+04	60.0	56.3	63.7
2.95E+04	1.59E+04	1.37E+04	86.6	86.8	86.4

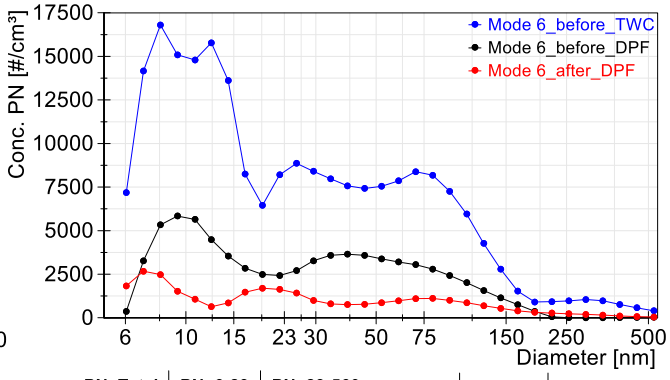

PN_Total [#/cm³]	PN_6-23 [#/cm³]	PN_23-560 [#/cm³]	Eff. Total [%]	Eff. 6-23 [%]	Eff. 23-560 [%]
2.49E+05	1.17E+05	1.31E+05	48.9	57.6	41.1
1.27E+05	4.97E+04	7.74E+04	64.5	64.2	64.6
4.52E+04	1.78E+04	2.74E+04	81.8	84.8	79.2

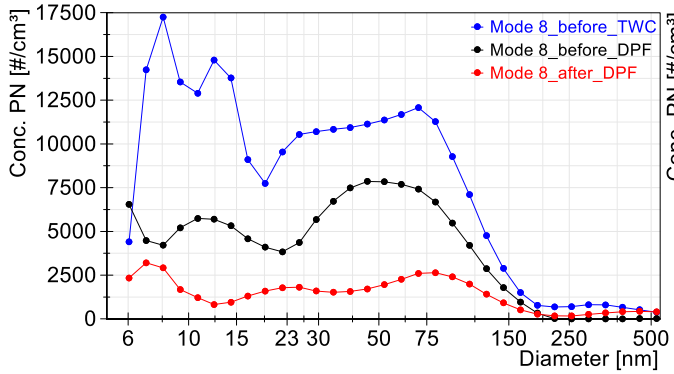

PN_Total [#/cm³]	PN_6-23 [#/cm³]	PN_23-560 [#/cm³]	Eff. Total [%]	Eff. 6-23 [%]	Eff. 23-560 [%]
3.60E+05	1.98E+05	1.62E+05	72.5	77.4	66.4
9.90E+04	4.47E+04	5.43E+04	58.6	47.8	67.5
4.10E+04	2.33E+04	1.77E+04	88.6	88.2	89.1

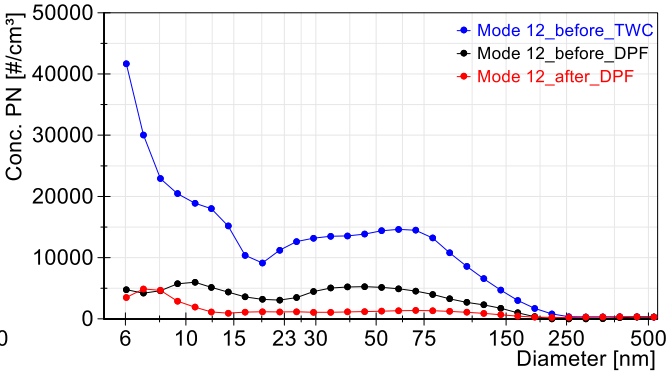

(A). Modes of low load

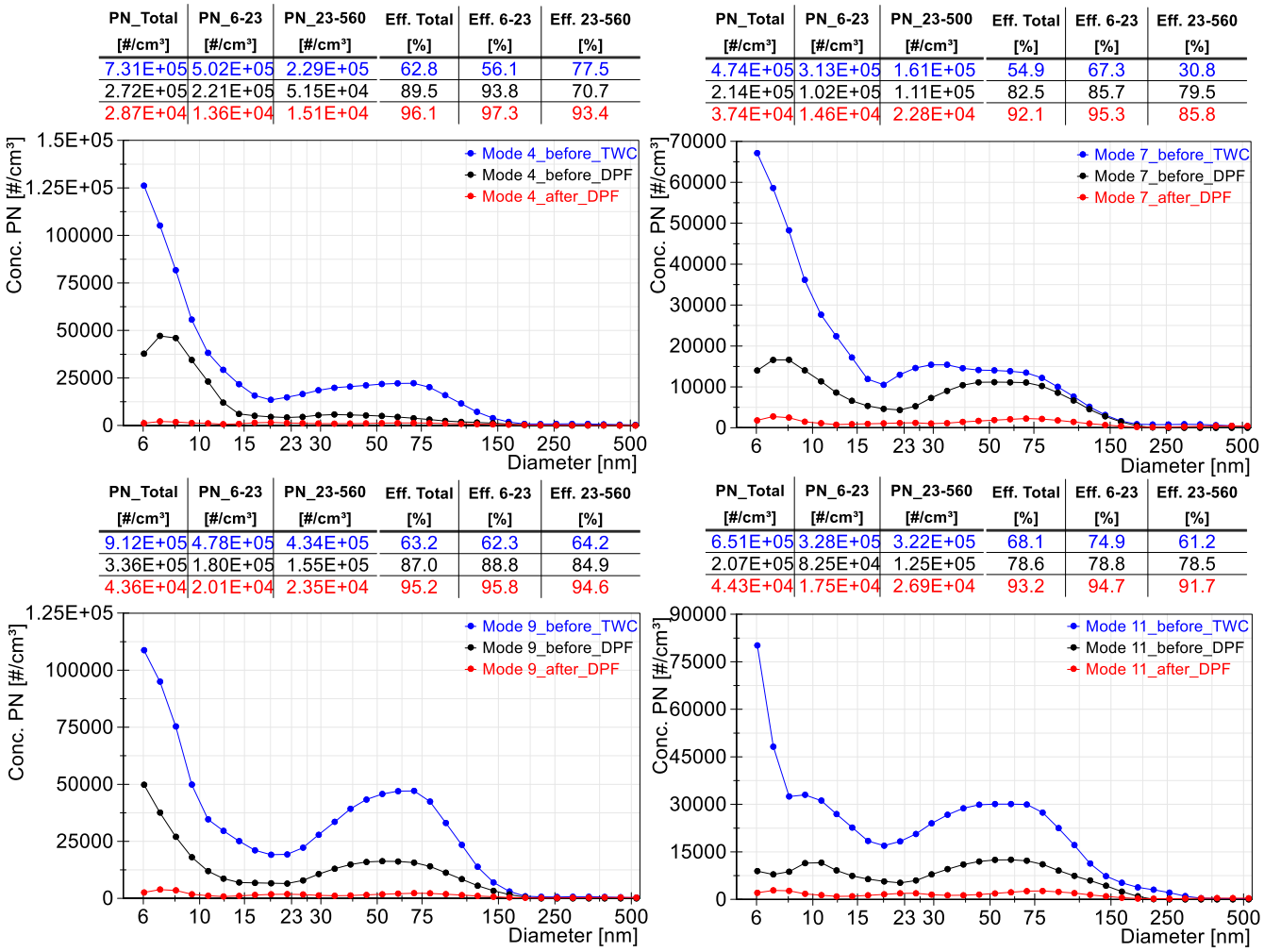

(B). Modes of medium and high load

Fig. 8. PM concentration, PSD, and efficiency of the ATS during steady-state modes of the engine

As noted above, the TSI-EEPS was used to measure PM concentration and PSD shown in graphs and charts of Figure 8, thanks to its 32 measure channels that allow to measure and gather particles of different sizes in a range of 6 nm to 560 nm. Two sets were employed to analyze the behaviors of PM emissions, as well as the efficiencies of TWC and DPF and their combined effects on PM emissions. The first and second sets pertain, respectively, to particles with diameters of less than and greater than 23 nm. The Euro VI code regulates only particles of the latter set.

PM emissions of the low load modes were generally less than those of modes with a higher and medium load. In addition to presenting high emission of particles with diameters of less than 23 nm, also showed an efficiency of greater than 92% of the ATS for all operating modes. Although DPF efficiency was greatest in most operating modes, the TWC effects on PM in the majority of operating modes studied nonetheless exceed 60%. This is due to the difference between the behavior of gaseous emissions as functions of temperature changes. where the first two staying in the gaseous phase when the exhaust gas temperature decreases, unlike UHC emissions composed of compounds semi-volatiles that can be converted in particles of the nucleation-mode with the decrease of exhaust gas temperature across the exhaust line[45]. For this reason, TWCs with efficiencies of greater than 97% for UHC reductions affect PM emissions mostly for particles of less than 23 nm in diameter.

3.3 Results for transient-state engine conditions

The results of pollutant emission evaluations across the exhaust gas line during the WHTC appear below, along with measures of ATS efficiency and its effect on each pollutant emission that was evaluated.

3.3.1. Results for gaseous compound emissions

Figure 9 shows emissions of CO, NOx, and UHC during WHTC cycle across the three points of the exhaust line. This information is used to study those three gaseous compounds' effects on TWC and DPF.

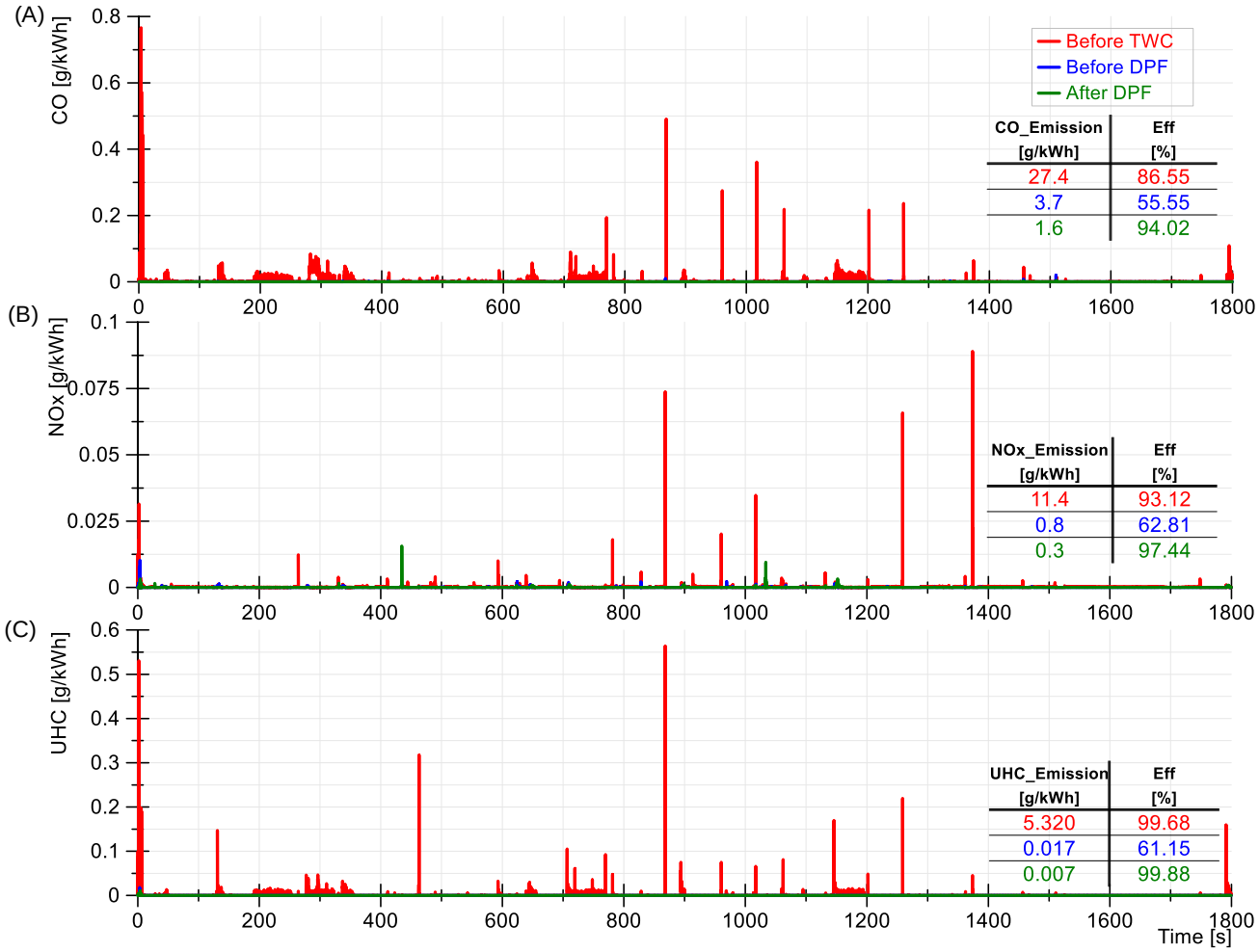

Fig. 9. Gaseous emissions and ATS efficiencies across three positions of the exhaust line during the WHTC.

Figure 9 shows ATS effects on the emissions of the three gaseous compounds, along with its influence so that the engine meets with the limits stipulated by the Euro VI regulation, which are 3.08 [g/kWh] for CO, 0.4 [g/kWh] for NOx, and 0.11 [g/kWh] for UHC. As in the steady-state study, the TWC's performance of efficiency of 99.68% was higher in UHC emissions than for in the other two gaseous compounds, with efficiencies of 86.55% for CO emissions and 93.12% for NOx emissions. These results corroborate those of *Tien et al*[46], which confirm that the TWC is the best alternative for reductions of CO, NOx, and UHC emissions from SI engines.

3.3.2. Results for particulate matter emissions

This section shows results for PM emissions during the WHTC in the three points along the exhaust gas line. This information is implicated in ATS's effects. Firstly, it is submitted in the analysis of the results obtained with the Horiba OBS ONE PM (Figure 10) that allows evaluating the emission of particles with diameters greater than 23 nm that are regulated by the Euro VI standard and subsequently the findings are analyzed with the TSI-EEPS 3090, an instrument that allows evaluating particles with diameters from 6 nm to 560 nm (Figure 11).

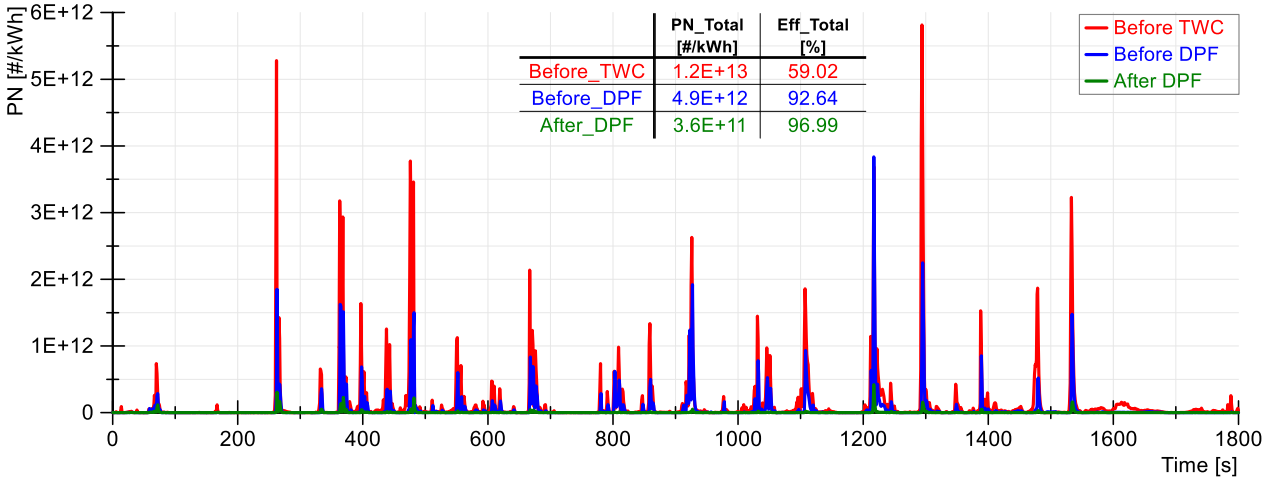

Fig. 10. Particle concentrations as measured with Horiba OBS-ONE during the WHTC.

Figure 10 shows how the engine complies with the Euro VI standard of 6·1011 [# / kWh] for PM emissions, owing to the implementation of the ATS. Although the DPF's efficiency of 92.64% allows to reduce engine PM emissions to comply with Euro VI limits, the TWC shows to have an influence on the reduction of PM emissions at a 59.02% efficiency. This corroborates results presented by others researches such as *Liu et al*[45] and *Di iorio et al*[47] that show a relationship between UHC and PM formation as well as TWC effects on PM reduction for particles from nucleation-mode.

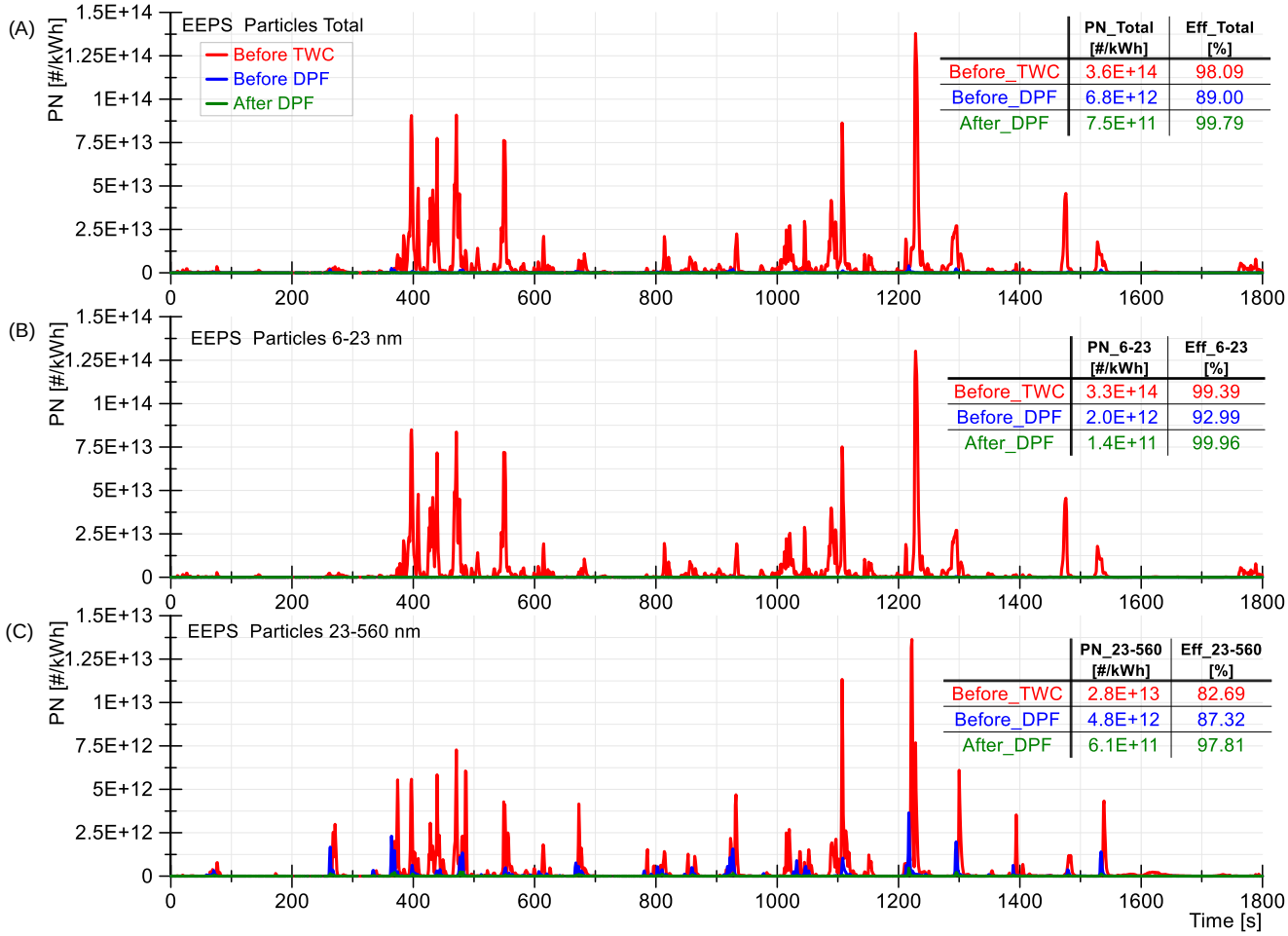

Fig. 11. Particle concentration measured with TSI-EEPS 3090 during the WHTC

Finally, Figure 11 presents the results obtained when evaluating PM emissions with the TSI-EEPS 3090 evaluating the same sets, total concentration (Figure 11A), particles with a diameter smaller than 23 nm (Figure

11B) and particles with diameters greater than 23 nm (Figure 11C), evaluated during the analysis of the stable states of the engine. It can be observed that, in general, the behavior of the emissions was similar to that observed with the results of the Horiba OBS ONE PM. However, it should be pointed out that when particles with diameters of less than 23 nm are considered, the efficiency of the TWC increases, which allows to observe that its efficiency in reducing this type of particles is 99.39%.

4. Conclusions

The purpose of this work has been to investigate the effects of TWC and DPF on pollutant emissions from an LPG-fueled engine. In this sense, the cycles WHSC and WHTC were employed to analyze pollutant emission behavior on steady and transient engine states; that thanks to after-treatment system implementation approved the EURO VI legislation.

Catalysts and PM filters are not a new topic in engines fueled with conventional fuels, where increasingly stringent regulations make the implementation of these systems common. However, this paper features after-treatment systems' influence on pollutant emissions from engines powered by alternative fuels whose emissions are less than those of engines powered by gasoline or diesel. The main work findings are described below:

- Transient state analyses showed a relationship between changes in engine load and emissions of gas-phase compounds. CO, UHC, and NOx emissions increase or decrease depending on the engine load changes, as observed in the WHTC trials. Nonetheless, emission behavior was different among these compound emissions when the steady-state points were studied. For example, modes 4 and 7 of the WHSC have relatively higher loads than the other modes. They had increased NOx and UHC emissions, but lower CO emissions. TWC has the greatest efficiency with a 99% reduction of UHC emissions in both steady and transient states.
- PM emission analysis shows the influence of ATS elements on these emissions. It should be noted that the measurement range between OBS and EEPS are completely different, thus, it is not possible to make a comparison between both instruments. Despite the aforementioned, results analyzed, they allowed observing as the particle filter is the element that takes care of the engine comply with current regulations, but the main finding of this work is the TWC influence on particle reduction, mainly those with large sizes less than 23nm.
- TWC is established as the device responsible for the reduction of small particles, and this aspect is linked to the effect of this device on volatile UHCs. This conclusion has been reached after analyzing the effects of this device in the reduction of UHC with an efficiency of 99%, considering that the efficiency in the reduction of small particles (diameter smaller than 23 nm) before and after catalyst was similar to UHC reduction.

Declaration of conflicting interests

The author(s) declared no potential conflicts of interest with respect to the research, authorship and/or publication of this article.

References

1. Awad OI, Ma X, Kamil M, et al. Particulate emissions from gasoline direct injection engines: A review of how current emission regulations are being met by automobile manufacturers. *Sci Total Environ* 2020; 718: 137302.
2. Hooftman N, Messagie M, Van Mierlo J, et al. A review of the European passenger car regulations – Real driving emissions vs local air quality. *Renew Sustain Energy Rev* 2018; 86: 1–21.
3. Huang G, Li Z, Zhao W, et al. Effects of fuel injection strategies on combustion and emissions of intelligent charge compression ignition (ICCI) mode fueled with methanol and biodiesel. *Fuel* 2020; 274: 117851.
4. Bermúdez V, Ruiz S, Novella R, et al. Assessment of air management strategies on particulate number and size distributions from a 2-stroke compression-ignition engine operating with gasoline Partially Premixed Combustion concept. *Int J Engine Res* 2020; 21: 448–469.
5. Ghaffarzadeh S, Nassiri Toosi A, Hosseini V. An experimental study on low temperature combustion in a light duty engine fueled with diesel/CNG and biodiesel/CNG. *Fuel* 2020; 262: 116495.

6. Pastor J V., García-Oliver JM, Micó C, et al. Experimental study of the effect of hydrotreated vegetable oil and oxymethylene ethers on main spray and combustion characteristics under engine combustion network spray A conditions. *Appl Sci*; 10. Epub ahead of print 2020. DOI: 10.3390/APP10165460.

7. Ren Y, Lou D, Tan P, et al. Emission reduction characteristics of after-treatment system on natural gas engine: Effects of platinum group metal loadings and ratios. *J Clean Prod* 2021; 298: 126833.

8. Lou D, Ren Y, Li X, et al. Effect of operating conditions and TWC parameters on emissions characteristics of a stoichiometric natural gas engine. *Energies*; 13. Epub ahead of print 2020. DOI: 10.3390/en13184905.

9. Napolitano P, Alfè M, Guido C, et al. Particle emissions from a HD SI gas engine fueled with LPG and CNG. *Fuel* 2020; 269: 117439.

10. Sharma N, Agarwal AK. Effect of Fuel Injection Pressure and Engine Speed on Performance, Emissions, Combustion, and Particulate Investigations of Gasohols Fuelled Gasoline Direct Injection Engine. *J Energy Resour Technol*; 142. Epub ahead of print 1 April 2020. DOI: 10.1115/1.4044763.

11. Zhang X, Pan L, Wang L, et al. Review on synthesis and properties of high-energy-density liquid fuels: Hydrocarbons, nanofluids and energetic ionic liquids. *Chem Eng Sci* 2018; 180: 95–125.

12. Zhang YC, Nie J, Cao J, et al. Synthesis of high-density flammable hydrocarbon as potential hypergolic fuel and ignition additive of high-density fuels. *Combust Flame* 2020; 222: 252–258.

13. Ramalingam S, Mahalakshmi N V. Influence of high pressure fuel injection system on engine performance and combustion characteristics of Moringa Oleifera biodiesel and its blends. *Fuel* 2020; 279: 118461.

14. Simsek S, Uslu S. Investigation of the impacts of gasoline, biogas and LPG fuels on engine performance and exhaust emissions in different throttle positions on SI engine. *Fuel* 2020; 279: 118528.

15. Nguyen Duc K, Nguyen Duy V, Hoang-Dinh L, et al. Performance and emission characteristics of a port fuel injected, spark ignition engine fueled by compressed natural gas. *Sustain Energy Technol Assessments* 2019; 31: 383–389.

16. Zhang Q, Li Z, Wei Z, et al. Experiment investigation on the emission characteristics of a stoichiometric natural gas engine operating with different reference fuels. *Fuel* 2020; 269: 117449.

17. Gürbüz H, Şöhret Y, Akçay H. Environmental and enviroeconomic assessment of an LPG fueled SI engine at partial load. *J Environ Manage* 2019; 241: 631–636.

18. Mohammed HA, Abdulhaleem SM. Experimental Study of Spark Ignition Engine Operated with Naphtha or Gasoline Blended LPG Fuel. *Bull Fac Eng Mansoura Univ* 2020; 41: 9–17.

19. Xu Y, Zhang Y, Gong J, et al. Combustion behaviours and emission characteristics of a retrofitted NG/gasoline duel-fuel SI engine with various proportions of NG-gasoline blends. *Fuel* 2020; 266: 116957.

20. Rood S, Eslava S, Manigrasso A, et al. Recent advances in gasoline three-way catalyst formulation: A review. *Proc Inst Mech Eng Part D J Automob Eng* 2020; 234: 936–949.

21. Meng Z, Li J, Fang J, et al. Experimental study on regeneration performance and particle emission characteristics of DPF with different inlet transition sections lengths. *Fuel* 2020; 262: 116487.

22. McCaffery C, Zhu H, Li C, et al. On-road gaseous and particulate emissions from GDI vehicles with and without gasoline particulate filters (GPFs) using portable emissions measurement systems (PEMS). *Sci Total Environ* 2020; 710: 136366.

23. Distaso E, Amirante R, Tamburrano P, et al. Particle emissions from a HD SI gas engine fueled with LPG and CNG. *Appl Energy* 2020; 269: 671–678.

24. Macor A, Benato A. Regulated Emissions of Biogas Engines—On Site Experimental Measurements and Damage Assessment on Human Health. *Energies* 2020; 13: 1044.

25. Boothe VL, Baldauf RW. *Traffic emission impacts on child health and well-being*. Elsevier Inc. Epub ahead of print 2019. DOI: 10.1016/B978-0-12-814694-1.00007-5.

26. Piloto-Rodríguez R, Díaz Y, Melo-Espinosa EA, et al. Conversion of fatty acid distillates into biodiesel: engine performance and environmental effects. *Energy Sources, Part A Recover Util Environ Eff* 2020; 42: 387–398.

27. Chan JH, Tsolakis A, Herreros JM, et al. Combustion, gaseous emissions and PM characteristics of Di-Methyl Carbonate (DMC)-gasoline blend on gasoline Direct Injection (GDI) engine. *Fuel* 2020; 263: 116742.

28. Dappe V, Uzu G, Schreck E, et al. Single-particle analysis of industrial emissions brings new insights for health risk assessment of PM. *Atmos Pollut Res* 2018; 9: 697–704.

29. Wang D, Li Q, Shen G, et al. Significant ultrafine particle emissions from residential solid fuel combustion. *Sci Total Environ* 2020; 715: 1–7.

30. Ghadikolaei MA, Yung KF, Cheung CS, et al. Non-polar organic compounds, volatility and oxidation reactivity of particulate matter emitted from diesel engine fueled with ternary fuels in blended and fumigation modes. *Chemosphere* 2020; 249: 126086.

31. Wang P, Gu W, Lei L, et al. Micro-structural and components evolution mechanism of particular matter from diesel engines with non-thermal plasma technology. *Appl Therm Eng* 2015; 91: 1–10.

32. Wu B, Deng L, Gu W, et al. Experimental investigation of combustion and particle emissions under different combustion modes on a heavy-duty diesel engine fueled by diesel/gasoline/diesel from direct coal liquefaction. *Fuel*; 254. Epub ahead of print 2019. DOI: 10.1016/j.fuel.2019.115661.

33. Sirignano M, Conturso M, Magno A, et al. Evidence of Sub-10 nm Particles Emitted from a Small-size Diesel Engine. *Exp Therm Fluid Sci* 2018; 95: 60–64.

34. Desantes JM, Bermúdez V, Molina S, et al. Methodology for measuring exhaust aerosol size distributions using an engine test under transient operating conditions. *Meas Sci Technol* 2011; 22: 115101.

35. Seinfeld JH, Pandis SN. *Atmospheric chemistry and physics: from air pollution to climate change*. John Wiley & Sons, 2016.

36. Gong J, Pihl J, Wang D, et al. O2 dosage as a descriptor of TWC performance under lean/rich dithering in stoichiometric natural gas engines. *Catal Today* 2020; 1–11.

37. Tan P qiang, Duan L shuang, Li E feng, et al. Experimental study on the temperature characteristics of a diesel particulate filter during a drop to idle active regeneration process. *Appl Therm Eng* 2020; 178: 115628.

38. Li L, Yu Y, Lin W. Numerical investigation on the effects of load conditions and hydrogen-air ratio on the combustion processes of a HSDI engine. *Int J Hydrogen Energy* 2020; 45: 10602–10612.

39. Yang Z, Miganakallu N, Miller T, et al. Investigation of high load operation of spark-ignited over-expanded Atkinson cycle engine. *Appl Energy* 2020; 262: 114519.

40. Soto Izquierdo L. *Estudio del efecto de diferentes estrategias de formación de la mezcla sobre las emisiones gaseosas y de partículas en nuevos conceptos de combustión de motores de encendido por compresión*. Universitat Politècnica de València. Epub ahead of print 28 July 2020. DOI: 10.4995/Thesis/10251/149401.

41. Shu J, Fu J, Liu J, et al. Influences of excess air coefficient on combustion and emission performance of diesel pilot ignition natural gas engine by coupling computational fluid dynamics with reduced chemical kinetic model. *Energy Convers Manag* 2019; 187: 283–296.

42. Sakai M, Hamaguchi T, Tanaka T. Improving high-temperature NOx conversion in the combined NSR-SCR system with an SCR catalyst mixed with an NH3 adsorbent. *Appl Catal A Gen* 2019; 582: 117105.

43. Kai X, Meng Y, Yang T, et al. Effect of torrefaction on rice straw physicochemical characteristics and particulate matter emission behavior during combustion. *Bioresour Technol* 2019; 278: 1–8.

44. Yontar AA, Doğu Y. Effects of equivalence ratio and CNG addition on engine performance and emissions in a dual sequential ignition engine. *Int J Engine Res* 2020; 21: 1067–1082.

45. Liu H, Li Z, Xu H, et al. Nucleation mode particle evolution in a gasoline direct injection engine

with/without a three-way catalyst converter. *Appl Energy*; 259. Epub ahead of print 2020. DOI: 10.1016/j.apenergy.2019.114211.

46. Tien ND, Quang KV, Luong NT, et al. Study on improving emission conversion efficiency of three-way catalyst equipped in carburetor motorcycle by air supplement system. *Int J Ambient Energy* 2020; 1–9.

47. Di Iorio S, Catapano F, Magno A, et al. Investigation on sub-23 nm particles and their volatile organic fraction (VOF) in PFI/DI spark ignition engine fueled with gasoline, ethanol and a 30 %v/v ethanol blend. *J Aerosol Sci* 2020; 105723.

Definitions/Abbreviations

CI	compression ignition
CO	carbon monoxide
CO2	carbon dioxide
DPF	diesel particle filter
EEPS	engine exhaust particle sizer
GPF	gasoline particle filter
HD	heavy dutty
UHC	unburne hydrocarbons
ICE	internal combustion engine
LPG	liquified petroleum gas
NOx	nitrogen oxides
OBS	onboard system
PN	particle number
PM	particle matter
PSD	particle size distribution
SI	spark ignition
TWC	three way catalyst
WHSC	world harmonized stationary cycle
WHTC	world harmonized transient cycle